Turing instability and traveling fronts for a nonlinear reaction-diffusion system with cross-diffusion

G. Gambino [a] M. C. Lombardo [a] M. Sammartino [a,*]

[a] *University of Palermo, Department of Mathematics and Computer Science Via Archirafi 34, 90123 Palermo, Italy.*

Abstract

In this work we investigate the phenomena of pattern formation and wave propagation for a reaction-diffusion system with nonlinear diffusion. We show how cross-diffusion destabilizes uniform equilibrium and is responsible for the initiation of spatial patterns. Near marginal stability, through a weakly nonlinear analysis, we are able to predict the shape and the amplitude of the pattern. For the amplitude, in the supercritical and in the subcritical case, we derive the cubic and the quintic Stuart-Landau equation respectively.

When the size of the spatial domain is large, and the initial perturbation is localized, the pattern is formed sequentially and invades the whole domain as a traveling wavefront. In this case the amplitude of the pattern is modulated in space and the corresponding evolution is governed by the Ginzburg-Landau equation.

Key words: Nonlinear diffusion, Turing bifurcation, Pattern formation, Amplitude equation, Quintic Stuart-Landau equation, Ginzburg-Landau equation, Traveling fronts.

1 Introduction

The emergence of ordered structures (patterns) is a phenomenon frequently observed in the physical world. Two different mechanisms which lead to pattern formation are known: self-assembly and self-organization. Self-assembly is

* Corresponding author.
Email addresses: gaetana@math.unipa.it (G. Gambino), lombardo@math.unipa.it (M. C. Lombardo), marco@math.unipa.it (M. Sammartino).

typical of spontaneous processes tending towards equilibrium. It is associated with the minimization of a variational energy functional in a closed system and the resulting pattern can survive indefinitely without external energy input [32]. On the other hand self-organization implies a far from equilibrium process, and is possible only in open system with an external energy source. Prototype models of self-organization generated patterns are the reaction-diffusion systems that, since the seminal paper of Turing [47], have attracted a growing interest as they constitute an essential basis to describe morphogenetic mechanisms.

Turing suggested that in a reaction-diffusion system describing the interaction between two species (or reactants), different diffusion rates can lead to the destabilization of a constant steady state, followed by the transition to a nonhomogeneous steady state. According to this result, a steady state is Turing unstable if it is stable as a solution to the reaction system (without diffusion terms), but unstable as a solution of the full reaction-diffusion system [28,39]. This mechanism, known as diffusion driven instability, leads to the pattern appearance.

Most of the reaction-diffusion systems used to predict the occurrence of patterns assume that the diffusion of each species depends only on the gradients of the concentration of the species itself. Nevertheless cross-diffusion terms (together with self-diffusion terms) should be introduced when the gradient of the density of one species induces a flux of another species, other than of the species itself. Self- and cross- diffusion terms were originally introduced in the context of population dynamics [37] and have now gained a renewed interest: they have appeared in various models arising in diverse contexts like chemotaxis [34], ecology [26,45,52], social systems [18,51], turbulent transport in plasmas [17,16], drift-diffusion in semiconductors [10,6,15], granular materials [3,21] and cell division in tumor growth [43], to name a few. However most of the papers where self- and cross- diffusion are considered focus on the mathematical properties of the system rather than on the pattern formation process. The importance of the cross-diffusion, relatively to pattern formation, is extensively discussed in [1,49] from both the experimental and the theoretical point of view. In these papers the authors report many experiments of interest to chemists where cross-diffusion effects can be quite significant: they obtain the minimal conditions for pattern formation in the presence of linear cross-diffusion terms, demonstrating that relatively small values of cross-diffusion parameters can lead to spatiotemporal pattern formation provided that the kinetics is sufficiently nonlinear.

The aim of this paper is to study the patterns admitted by the following strongly coupled reaction-diffusion system, where both nonlinear self- and

cross-diffusion terms are included:

$$\begin{aligned}\frac{\partial u}{\partial t} =&\boldsymbol{\nabla}\cdot\boldsymbol{J}_1+\Gamma u(\mu_1-\gamma_{11}u-\gamma_{12}v),\\ \frac{\partial v}{\partial t} =&\boldsymbol{\nabla}\cdot\boldsymbol{J}_2+\Gamma v(\mu_2-\gamma_{21}u-\gamma_{22}v)\ ,\end{aligned}\tag{1.1}$$

and the fluxes $\boldsymbol{J}_i$ have the following expression:

$$\begin{aligned}\boldsymbol{J}_1 =&\boldsymbol{\nabla}\left[u\left(c_1+a_1u+bv\right)\right]\ ,\\ \boldsymbol{J}_2 =&\boldsymbol{\nabla}\left[v\left(c_2+a_2v+b_2u\right)\right]\ .\end{aligned}\tag{1.2}$$

In (1.1) $u(\boldsymbol{x},t)$ and $v(\boldsymbol{x},t)$ with $\boldsymbol{x}\in\Omega$, $\Omega\subseteq\mathbb{R}^n$ are the population densities of two competing species. The nonlinear diffusion models the tendency of a species to diffuse (faster than predicted by the usual linear diffusion) towards lower density areas. The parameters $a_i\geq 0$ and $c_i\geq 0$ are respectively the self-diffusion and the diffusion coefficients, while the parameters b and b_2, the cross-diffusion coefficients, are both nonnegative being the species in a competitive relationship.

The constants $\gamma_{ij}>0$ represent the competitive interaction coefficients and the parameter Γ gives the relative strength of reaction terms (or, alternatively, the size of the spatial domain and the time scale). Initial conditions and boundary conditions must be added to the system (1.1). In this paper we are interested in self-organizing patterns and we shall impose the homogeneous Neumann boundary conditions which impose the weakest constraint on pattern formation. Moreover we shall treat the $1D$ case $\Omega=[0,2\pi]$.

Equations (1.1) were introduced by Shigesada, Kawasaki and Teramoto in [44] to model segregation effects, i.e. the possibility for a competing species to create a spatial niche. This effect, for competing species, is ruled out when cross- and self-diffusion are absent. In fact, when the diffusion is just the classical linear diffusion, and the domain Ω is convex, it can be proved ([31], see also [30] and references therein) that the only stable equilibrium solutions are spatially homogeneous. Since then the mathematical properties of the system (1.1) have been extensively studied, the main interest being on existence and stability of non constant steady solutions (see e.g. [35,36]), on existence and regularity of the solutions of the time dependent problem (see e.g. [8,9]), and on numerical schemes [20,4,25,2,7]. See also the interesting model in [22] where the system (1.1) is coupled with a transport law, and [19].

Recently it has been proposed a three-species model [30] with linear diffusion that, in the appropriate limit [11], shows convergence to (1.1).

The conditions for Turing instability for the system (1.1) were derived in [24,46,2]. In these papers it is shown that with a nonlinear diffusion of the

type given in (1.1), the simple Lotka-Volterra kinetics is sufficient to generate patterns. To the best of our knowledge no previous result which predicts the form and the amplitude of the pattern for the given system has been obtained. Our analysis will be mainly based on a weakly nonlinear analysis near equilibrium; we shall see that near the onset the development of the instabilities can be described in terms of the evolution in time of the amplitudes of the unstable normal mode [33]. A perturbation scheme will be applied to obtain the amplitude equation which takes into account the effect of the nonlinear terms in the resulting pattern (a complete review of the method can be found in [13]).

The plan of the paper is the following. In Section 2 we shall carry out a linear stability analysis of the coexistence equilibrium showing how the cross-diffusion is the key mechanism of pattern formation. In Section 3, through a weakly nonlinear multiple scale analysis, we shall derive the Stuart-Landau equation ruling the evolution of the amplitude of the most unstable mode. We analyze both the supercritical and the subcritical case. In the last case, to correctly describe the amplitude of the pattern, the weakly nonlinear analysis has to be pushed up to fifth order to finally derive the quintic Stuart-Landau equation. This equation is also able to describe the phenomenon of hysteresis one can observe in the subcritical case. In Section 4 we shall address the process of pattern formation when the size of the spatial domain is large. In this case we show how the pattern invades the spatial domain as a traveling wavefront. We shall derive the equation governing the amplitude of the pattern, the real Ginzburg-Landau equation, whose solution gives, to a good approximation, the shape and the speed of the traveling front.

For numerical simulation we have used an explicit (in time) spectral method or the particle method derived in [25]. All the numerical results show a good agreement with the solution prescribed by the weakly nonlinear expansion.

2 Turing instability

In this section we shall investigate, for the system (1.1), the possibility of pattern appearance. Through a linear stability analysis we shall show that the coexistence equilibrium is stable for the kinetic part of the system (1.1), but unstable for the full reaction-diffusion system. The analysis of the other equilibria can be found in [24].

The coexistence steady state:

$$(u_0, v_0) \equiv \left(\frac{\mu_1\gamma_{22} - \mu_2\gamma_{12}}{\gamma_{11}\gamma_{22} - \gamma_{12}\gamma_{21}}, \frac{\mu_2\gamma_{11} - \mu_1\gamma_{21}}{\gamma_{11}\gamma_{22} - \gamma_{12}\gamma_{21}} \right)$$

is a stable equilibrium point if $\gamma_{11}\gamma_{22} - \gamma_{12}\gamma_{21} > 0$, which corresponds to the weak interspecific competition case. In this paper we shall always assume the stability of (u_0, v_0). Moreover, for the point (u_0, v_0) to be a biologically significant steady state, the conditions $\mu_1\gamma_{22} - \mu_2\gamma_{12} > 0$ and $\mu_2\gamma_{11} - \mu_1\gamma_{21} > 0$ are imposed.

The linearized system in the neighborhood of (u_0, v_0) is:

$$\dot{\mathbf{w}} = \Gamma K \mathbf{w} + D\nabla^2 \mathbf{w} \,, \qquad\qquad \mathbf{w} \equiv \begin{pmatrix} u - u_0 \\ \\ v - v_0 \end{pmatrix} \,, \tag{2.1}$$

where we have defined:

$$K = \begin{pmatrix} -\gamma_{11}u_0 & -\gamma_{12}u_0 \\ \\ -\gamma_{21}v_0 & -\gamma_{22}v_0 \end{pmatrix} \,, \quad D = \begin{pmatrix} c_1 + 2a_1u_0 + bv_0 & bu_0 \\ \\ b_2v_0 & c_2 + 2a_2v_0 + b_2u_0 \end{pmatrix}. \tag{2.2}$$

Looking for solutions of system (2.1) of the form $e^{ikx+\lambda t}$ leads to the following dispersion relation, which gives the eigenvalue λ as a function of the wavenumber k:

$$\lambda^2 + (k^2 \operatorname{tr}(D) - \Gamma \operatorname{tr}(K))\lambda + h(k^2) = 0 \,, \tag{2.3}$$

where

$$h(k^2) = \det(D)k^4 + \Gamma q k^2 + \Gamma^2 \det(K) \,, \tag{2.4}$$

with:

$$\begin{aligned} q = {} & \gamma_{11}u_0(2a_2v_0 + c_2) + \gamma_{22}v_0(2a_1u_0 + c_1) + bv_0(\gamma_{22}v_0 - \gamma_{21}u_0) \\ & + b_2u_0(\gamma_{11}u_0 - \gamma_{12}v_0) \,. \end{aligned} \tag{2.5}$$

In what follows we shall derive the condition for pattern formation (2.8), the critical value for the bifurcation parameter (2.10), and the critical wavenumber (2.7).

Spatial patterns arise in correspondence of those modes k for which $Re(\lambda) > 0$ (see e.g. [38]). Since (u_0, v_0) is stable for the kinetics one has that $\operatorname{tr}(K) < 0$. Moreover one has that $\operatorname{tr}(D) > 0$. Therefore the only way to have $Re(\lambda) > 0$ for some $k \neq 0$ in (2.3) is when $h(k^2) < 0$. Thus, the condition for the marginal stability at some $k = k_c$ is:

$$\min(h(k_c^2)) = 0. \tag{2.6}$$

The minimum of h is attained when:

$$k_c^2 = -\frac{\Gamma q}{2\det(D)}, \tag{2.7}$$

which requires $q < 0$. The first two terms on the right hand side of expression (2.5) are non-negative: it follows that the only potential destabilizing

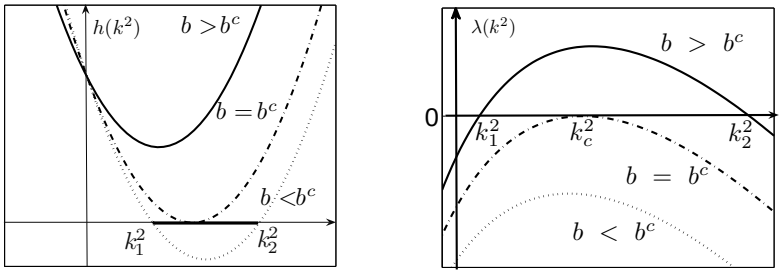

Fig. 2.1. *Left*: Plot of $h(k^2)$. *Right*: Growth rate of the k-th mode. A band of growing modes is present.

mechanism is the presence of the cross–diffusion terms. The conditions on the positiveness and stability of the equilibrium point (u_0, v_0) imply that only one of the two following inequalities can be satisfied:

$$\gamma_{22}v_0 - \gamma_{21}u_0 < 0 \qquad \text{or} \qquad \gamma_{11}u_0 - \gamma_{12}v_0 < 0. \tag{2.8}$$

Therefore when b has a destabilizing effect then b_2 acts as a stabilizer and vice versa. In what follows we shall choose the case $\gamma_{22}v_0 - \gamma_{21}u_0 < 0$ without loss of generality and b as the bifurcation parameter. Since the graph of $h(k^2)$ depends on b (see Fig. 2.1), from (2.6) one gets the bifurcation value of b (and the corresponding value of k_c^2). Defining the quantities α and β as:

$$\begin{aligned}
&\alpha = v_0(\gamma_{21}u_0 - \gamma_{22}v_0)\,,\\
&\beta = \gamma_{11}u_0(2a_2v_0 + c_2) + \gamma_{22}v_0(2a_1u_0 + c_1) + b_2u_0(\gamma_{11}u_0 - \gamma_{12}v_0)\,,
\end{aligned}$$

so that $q = -\alpha\, b + \beta$ and introducing in (2.6) $b = \beta/\alpha + \xi$ one gets:

$$\begin{aligned}
&\frac{\alpha^2}{4\det(K)}\,\xi^2 - v_0(2a_2v_0 + c_2)\xi \\
&\qquad -[v_0\beta/\alpha(2a_2v_0 + c_2) + (2a_1u_0 + c_1)(2a_2v_0 + b_2u_0 + c_2)] = 0,
\end{aligned} \tag{2.9}$$

whose positive root $\xi = \xi^+$ (this choice guarantees the condition $q < 0$) gives the critical value of the parameter b:

$$b^c = \beta/\alpha + \xi^+\,. \tag{2.10}$$

For $b > b^c$ the system has a finite k pattern-forming stationary instability. The unstable wavenumbers stay in between the roots of $h(k^2)$, denoted by k_1^2 and k_2^2, which are proportional to Γ [38]. Hence, to have the possibility of the pattern formation, Γ must be big enough so that at least one of the modes allowed by the boundary conditions falls within the interval $[k_1^2, k_2^2]$.

The region in the parameter space where the pattern can develop (i.e. the region where condition (2.8) is verified) is studied in Appendix A.

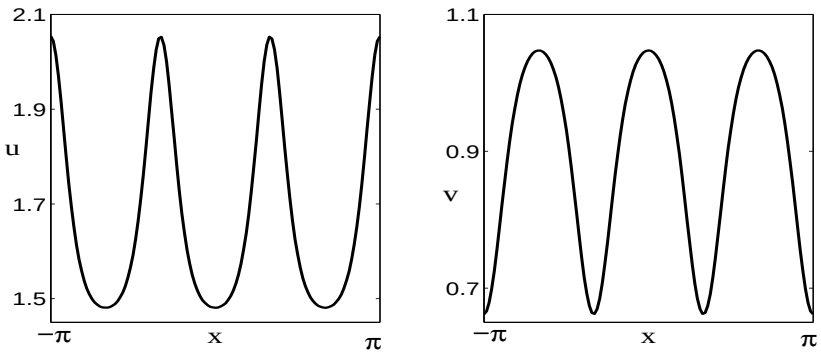

Fig. 2.2. The parameters are $\mu_1 = 1.2$, $\mu_2 = 1$, $\gamma_{11} = 0.5$, $\gamma_{12} = 0.4$, $\gamma_{21} = 0.38$, $\gamma_{22} = 0.41$, $a_1 = 10^{-4}$, $a_2 = 0.1$, $c_i = 0.2$, $\Gamma = 49.75$, $b_2 = 0.3$, $b = 6.5 > b^c = 5.297$.

In Fig. 2.2 we show the pattern which forms starting from an initial datum which is a random periodic perturbation of the equilibrium (u_0, v_0). The parameters we have picked for this simulation give $(u_0, v_0) \approx (1.74, 0.83)$ while the critical value of the bifurcation parameter is $b^c = 5.297$ and $k_c = 3.2$.

3 Weakly nonlinear analysis

The linear stability theory represents a useful first step in understanding pattern formation, but it gives only a rough indication of the patterns we should expect. Through the linear analysis we determine both the conditions on the system parameters for the onset of instability to infinitesimal disturbances and the length scale of the pattern formation $1/k_c$. Moreover the linear analysis displays the important physical processes and shows how the cross-diffusion is the key mechanism for the pattern formation.

Nevertheless the exponentially growing solutions obtained via the linear theory are physically meaningless. To predict the amplitude and the form of the pattern close to the threshold the nonlinear terms must be included into the analysis, and we shall perform a weakly nonlinear analysis based on the method of multiple scales. For a review see [50].

Since close to the bifurcation the amplitude of the pattern evolves on a slow temporal scale, new scaled coordinates are introduced which are treated as separate variables in addition to the original variables.

The solution of the original system (1.1) is written as a weakly nonlinear expansion in the small control parameter ε, representing the dimensionless distance from the threshold. Here we choose $\varepsilon^2 = (b - b^c)/b^c$. We shall see how the leading term of the nonlinear expansion of the solution is the product of the basic pattern (the critical solution of the linearized system (2.1)) and a

slowly varying amplitude (see [27,29]).

The slow scale is obtained from the linear analysis: for ε sufficiently small, it is straightforward to verify that $\lambda \sim \varepsilon^2$ and, since the growth rate of the perturbation is proportional to $e^{\lambda t}$, it follows that the characteristic time scale of evolution T is $O(\varepsilon^{-2})$. Near the bifurcation we separate the fast time t and slow time $T = \varepsilon^2 t$ and therefore the time derivative decouples as $\partial_t \to \partial_t + \varepsilon^2 \partial_T$.

At this stage we shall not consider the possibility of spatially modulated patterns and therefore, in our asymptotic expansion, we shall not include the spatial slow scale. This will be done in Section 4.

Separating the linear part and the nonlinear (in fact quadratic) part, we can recast the original system (1.1) in the following form:

$$\partial_t \mathbf{w} = \mathcal{L}^b \mathbf{w} + \frac{1}{2}\mathcal{Q}_K(\mathbf{w},\mathbf{w}) + \frac{1}{2}\nabla^2 \mathcal{Q}_D^b(\mathbf{w},\mathbf{w}), \tag{3.1}$$

where $\mathbf{w}$ is defined in (2.1). The linear operator $\mathcal{L}^b$ is defined as:

$$\mathcal{L}^b = \Gamma\, K + D^b \nabla^2, \tag{3.2}$$

where K and D^b are given in (2.2). Notice that here (for notational convenience) we are making explicit the dependence on the bifurcation parameter b. The action of the bilinear operators $\mathcal{Q}_K$ and $\mathcal{Q}_D^b$ on the couple $(\mathbf{x},\mathbf{y})$, where $\mathbf{x} = (x^u, x^v)$ and $\mathbf{y} = (y^u, y^v)$ is defined as:

$$\mathcal{Q}_K(\mathbf{x},\mathbf{y}) = \Gamma \begin{pmatrix} -2\gamma_{11}x^u y^u - \gamma_{12}(x^u y^v + x^v y^u) \\ -2\gamma_{22}x^v y^v - \gamma_{21}(x^u y^v + x^v y^u) \end{pmatrix}, \tag{3.3}$$

$$\mathcal{Q}_D^b(\mathbf{x},\mathbf{y}) = \begin{pmatrix} 2a_1 x^u y^u + b(x^u y^v + x^v y^u) \\ 2a_2 x^v y^v + b_2(x^u y^v + x^v y^u) \end{pmatrix}. \tag{3.4}$$

Passing to the asymptotic analysis, we expand b and $\mathbf{w}$ as:

$$b = b^c + \varepsilon^2 b^{(2)} + O(\varepsilon^4)\,, \tag{3.5}$$

$$\mathbf{w} = \varepsilon\, \mathbf{w}_1 + \varepsilon^2\, \mathbf{w}_2 + \varepsilon^3\, \mathbf{w}_3 + O(\varepsilon^4). \tag{3.6}$$

Moreover the linear operator $\mathcal{L}^b$ can be expanded as:

$$\mathcal{L}^b = \mathcal{L}^{b^c} + \varepsilon^2\, b^{(2)} \begin{pmatrix} v_0 & u_0 \\ 0 & 0 \end{pmatrix} \nabla^2 \,, \tag{3.7}$$

while:

$$\mathcal{Q}_K(\mathbf{w},\mathbf{w}) = \varepsilon^2 \mathcal{Q}_K(\mathbf{w}_1,\mathbf{w}_1) + 2\varepsilon^3 \mathcal{Q}_K(\mathbf{w}_1,\mathbf{w}_2) + O(\varepsilon^4), \tag{3.8}$$

$$\mathcal{Q}_D^b(\mathbf{w},\mathbf{w}) = \varepsilon^2 \left[\mathcal{Q}_D^{b^c}(\mathbf{w}_1,\mathbf{w}_1) + b^{(2)} \begin{pmatrix} u_0 v_0 \\ 0 \end{pmatrix} \right] + \tag{3.9}$$

$$\varepsilon^3 \left[2\mathcal{Q}_D^{b^c}(\mathbf{w}_1,\mathbf{w}_2) + b^{(2)} \begin{pmatrix} u_0 w_1^v + v_0 w_1^u \\ 0 \end{pmatrix} \right] + O(\varepsilon^4).$$

Substituting all the above expansions into (3.1) and collecting the terms at each order in ε, one gets a sequence of equations for the $\mathbf{w}_i$.

At the lowest order in ε we recover the linear problem $\mathcal{L}^{b^c}\mathbf{w}_1 = \mathbf{0}$ whose solution, satisfying the Neumann boundary conditions, is given by:

$$\mathbf{w}_1 = A(T)\boldsymbol{\rho}\cos(k_c x)\,, \qquad \text{with} \quad \boldsymbol{\rho} \in \mathrm{Ker}(\Gamma K - k_c^2 D^{b^c}) \tag{3.10}$$

where $A(T)$ is the amplitude of the pattern and it is still arbitrary at this level. The vector $\boldsymbol{\rho}$ is defined up to a constant and we shall make the normalization in the following way:

$$\boldsymbol{\rho} = \begin{pmatrix} 1 \\ M \end{pmatrix}, \qquad \text{with} \quad M \equiv \frac{-D_{21}^{b^c} k_c^2 + \Gamma K_{21}}{D_{22}^{b^c} k_c^2 - \Gamma K_{22}}, \tag{3.11}$$

where $D_{ij}^{b^c}, K_{ij}$ are the i,j-entries of the matrices D^{b^c} and K.

At $O(\varepsilon^2)$ and at $O(\varepsilon^3)$ one gets the following linear equations:

$$\mathcal{L}^{b^c}\mathbf{w}_2 = \mathbf{F}\,, \tag{3.12}$$

$$\mathcal{L}^{b^c}\mathbf{w}_3 = \mathbf{G}\,. \tag{3.13}$$

The explicit expression of $\mathbf{F}$ and $\mathbf{G}$ is given in the Appendix B. Since $\mathbf{F}$ is orthogonal to the kernel of the adjoint of $\mathcal{L}^{b^c}$, Eq.(3.12) can be solved right away.

This is not the case for the equation for $\mathbf{w}_3$. The solvability condition for this equation gives the Stuart-Landau equation for the amplitude $A(T)$:

$$\frac{dA}{dT} = \sigma A - LA^3, \tag{3.14}$$

where the coefficients σ and L are explicitly computed in terms of the system parameters. All the details are given in the Appendix B.

Since the growth rate coefficient σ is always positive, the dynamics of the Stuart-Landau equation (3.14) can be divided into two qualitatively different cases depending on the sign of the Landau constant L: the supercritical case, when L is positive, and the subcritical case, when L is negative (see also the discussion in the final part of Appendix B).

3.1 The supercritical case

If the coefficients σ and L, appearing into (3.14), are both positive, then there exists the stable equilibrium solution $A_\infty = \sqrt{\sigma/L}$, which represents the asymptotic value of the amplitude A. Therefore, we are now able to predict the amplitude and the form of the pattern. According to the weakly nonlinear theory the asymptotic (in time) behavior of the solution is given by:

$$\mathbf{w} = \varepsilon \boldsymbol{\rho} \sqrt{\frac{\sigma}{L}} \cos(k_c x) + \varepsilon^2 \frac{\sigma}{L} \left(\mathbf{w}_{20} + \mathbf{w}_{22} \cos(2k_c x)\right) + O(\varepsilon^3). \tag{3.15}$$

In the above expression $\boldsymbol{\rho}$ is given in (3.11), while the $\mathbf{w}_{2i}$ are the solutions of the systems (B.5).

Clearly, in general, the above solution is not compatible with the Neumann boundary conditions, that require k_c to be integer or semi-integer. We therefore define $\bar{k}_c$ as the first integer or semi-integer to become unstable when b passes the critical value b_c, and take as the weakly nonlinear approximation the following expression:

$$\mathbf{w} = \varepsilon \boldsymbol{\rho} \sqrt{\frac{\sigma}{L}} \cos\left(\bar{k}_c x\right) + \varepsilon^2 \frac{\sigma}{L} \left(\mathbf{w}_{20} + \mathbf{w}_{22} \cos\left(2\bar{k}_c x\right)\right) + O(\varepsilon^3). \tag{3.16}$$

In our numerical tests we have seen that the discrepancy between k_c and $\bar{k}_c$ does not ruin the accuracy of the approximation. In Fig. 3.1 we show the comparison between the stationary state (3.16) predicted by the weakly nonlinear analysis and the stationary state (reached starting from a random perturbation of the constant state) computed solving numerically the system (1.1). On the left we picked $\varepsilon \approx 0.316$. Please notice that we have chosen $b^{(2)} = b^c$, meaning that the deviation from the critical value b^c is measured

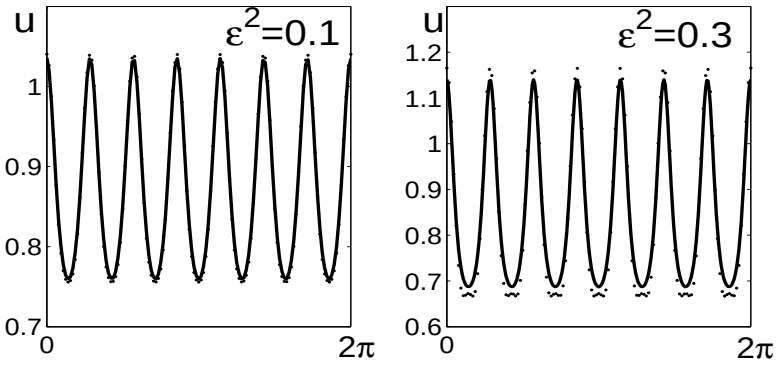

Fig. 3.1. Comparison between the weakly nonlinear solution (dotted line) and the numerical solution of (1.1) (solid line). The parameters are $\Gamma = 80$, $a_i = 10^{-4}$, $c_i = 0.2$ $b_2 = 0.3$, $\mu_1 = 1.0$, $\mu_2 = 1.2$, $\gamma_{11} = 1.0$, $\gamma_{12} = 0.3$, $\gamma_{21} = 0.93$, $\gamma_{22} = 1.0$. With this choice of the parameters one has $b^c \approx 7.377$, $u_0 \approx 0.89$, while $k_c \approx 6.98$. The first admissible unstable mode is $\bar{k}_c = 7$ *Left*: $\varepsilon^2 = 0.1$. *Right*: $\varepsilon^2 = 0.3$.

relative to the size of b^c. Therefore, for the aforementioned value of ε, one has that $b = 1.1 \times b^c$ where, for the parameters chosen in the Figure, $b^c = 7.377$.

On the right of Fig. 3.1 we show a similar comparison for a larger deviation from the bifurcation value, having picked $\varepsilon \approx 0.548$. The distance, evaluated in the L^1 norm, between the weakly nonlinear approximations and the numerical solutions of the system is about 5.5×10^{-3} when $\varepsilon \approx 0.316$, while it is $\approx 2.7 \times 10^{-2}$ when $\varepsilon \approx 0.548$. This is consistent with the weakly nonlinear solution being an $O(\varepsilon^3)$ approximation of the solution. A better approximation of the amplitude A of the pattern can be obtained by using the quintic Stuart-Landau equation (3.21) (the details of the analysis will be given in the next section). In Fig. 3.2 we show, for the rather large deviation for equilibrium $\varepsilon = 0.707$, a comparison between the numerical solution of the system (1.1) and the weakly nonlinear approximation at $O(\varepsilon^3)$, which shows a significant discrepancy from the solution, and the approximation at $O(\varepsilon^5)$ which, instead, is still quite accurate.

3.1.1 Competition of modes away from threshold

For higher values of the bifurcation parameter other modes, beside the $\bar{k}_c$, become unstable, see Fig. 3.3. The weakness of the approach based on amplitude equations (to any order of accuracy) to predict the amplitude of the pattern far from equilibrium is the implicit assumption that, even for larger deviations from the bifurcation value, when other modes different from $\bar{k}_c$ have a positive growth rate, $\bar{k}_c$ remains the fastest growing mode and, ultimately, the predominant mode in the solution.

In Fig. 3.3 (where we plot, for specific parameter values, the same quantity

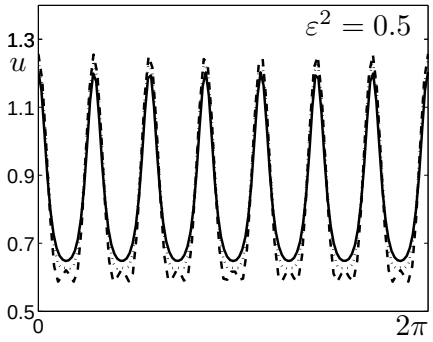

Fig. 3.2. Comparison between the weakly nonlinear solution, with the amplitude approximated at $O(\varepsilon^3)$ (dashed line) and at $O(\varepsilon^5)$ (dotted line), and the numerical solution of (1.1) (solid line). The parameter values are chosen as in Fig.3.1.

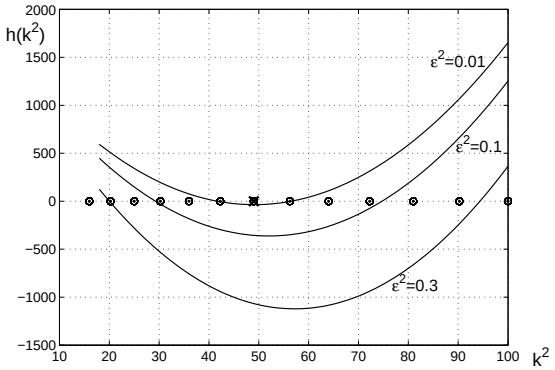

Fig. 3.3. The unstable modes are the integers and the semi-integers (marked with dots) for which $h(k^2) < 0$. The critical mode $\bar{k}_c$ is marked with a cross. The parameter values are the same of Fig. 3.1

$h(k^2)$ represented on the left of Fig. 2.1) one can see the unstable modes for different values of ε^2. For example, when $\varepsilon^2 = 0.3$ one has that all integers and semi-integers between $9/2$ and $19/2$ are unstable. And in fact one can see that, far enough from the bifurcation value b^c, there exist initial conditions for which one observes the development of patterns with different shapes. For each value of ε^2 we have run a thousand simulations (for the case $\varepsilon^2 = 0.7$ we run four thousands simulations), with different randomly chosen initial data. In Table 3.1 we report the percentages of the cases in which different shapes have emerged. We now show how the linear theory can give some clues on the wavelength of the emerging pattern (at least for values of ε that are not exceedingly large).

The first factor to be considered is the value k_m maximizing the growth rate $\lambda(k^2)$. Following the reasoning in [40] the value of k_m can be found by setting:

$$\frac{d\lambda^+}{dk^2} = 0, \tag{3.17}$$

Table 3.1

	$k = 11/2$	$k = 6$	$k = 13/2$	$\bar{\mathbf{k}}_\mathbf{c} = \mathbf{7}$	$k = 15/2$	$k = 8$
$\varepsilon^2 = 0.01$				100%		
$\varepsilon^2 = 0.1$			26%	62%	12%	
$\varepsilon^2 = 0.3$		4.6%	37.6%	44.3%	13.2%	0.3%
$\varepsilon^2 = 0.7$	0.1%	13.65%	42.725%	36.675%	6.825%	0.025%

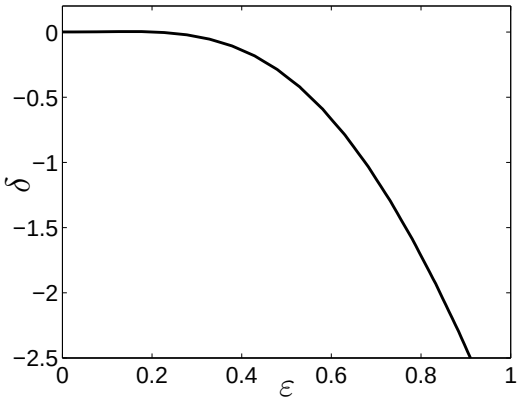

Fig. 3.4. The curve $d\lambda^+/dk^2 = 0$ once substituted $b = b^c(1 + \varepsilon^2)$ and $k_m^2 = k_c^2 + \delta$. The parameter values are chosen as in Fig.3.1.

where λ^+ is the positive root of the dispersion relation (2.3). Substituting $b = b^c(1+\varepsilon^2)$ and $k_m^2 = k_c^2+\delta$ in (3.17) one can obtain the analytic expression of the curve which gives δ as a function of ε. In Fig. 3.4 we represent the dependence of δ from ε, where all the other parameters are the same as in Fig. 3.1. In this case one can see that positive values of the parameter ε correspond to negative values of δ, i.e. k_m^2 always smaller than k_c^2. This could account for the bias on low wavenumbers of Table 3.1.

On the other hand, when nonlinear effects become significant, one has to take into account another important factor, other than the growth rate of each mode, namely its initial amplitude. In fact, intermode suppression comes into play: the growth of one mode tends to damp the growth of the others, as if they were competing. This implies that a mode of sufficiently dominant initial amplitude may extinguish modes with larger growth rates.

To describe the competition of the growing modes one can write a set of coupled ODEs governing the dynamics of the amplitudes. The problem of the derivation of these ODEs has been extensively addressed, in particular in the context of fluid dynamics. A complete discussion on the different methods developed for studying competing instabilities can be found in [12]. Here we shall follow the approach presented by Segel in [41] and [42]. Starting from

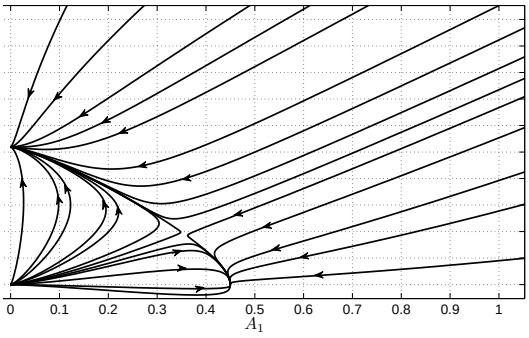

Fig. 3.5. The phase plane. The competitive modes are $k_1 = 6$ and $k_2 = \bar{k}_c$. The parameter values are the same of Fig. 3.1, $\varepsilon^2 = 0.7$.

the full system (1.1), we derive the following ODE model that illustrates the nonlinear interaction of the amplitudes A_1 and A_2 of two competing modes k_1 and k_2:

$$\frac{dA_1}{dT_2} = \sigma_1 A_1 - L_1 A_1^3 - \Omega_1 A_1 A_2^2 \,, \tag{3.18a}$$

$$\frac{dA_2}{dT_2} = \sigma_2 A_2 - L_2 A_2^3 - \Omega_2 A_1^2 \, A_2 \,, \tag{3.18b}$$

where the explicit expressions of the coefficients $\sigma_i > 0$ and L_i, Ω_i, with $i = 1, 2$ are given in Appendix D. In the experiment shown in Figures 3.5, 3.6 and 3.7 we consider the competition between two of the six modes admitted for $\varepsilon^2 = 0.7$, i.e. $k_1 = 6$ and $k_2 = 7$ (see Table 3.1). We see how the system (3.18a)-(3.18b) is able to predict the final evolution of the pattern. In the considered case, the system (3.18a)-(3.18b) admits no coexistence stable state and the system can evolve only toward one of the two stable states $(A_1, 0)$ and $(0, A_2)$. Therefore, this toy model for the intermode interaction predicts although the amplitudes of the modes k_1 and k_2, one ultimately becomes extinct, the crucial role being played by the initial conditions.

3.2 The subcritical case

For certain values of the parameters appearing in the Eqs. (1.1), we found that the Landau coefficient L has a negative value. Therefore Eq. (3.14) is not able to capture the amplitude of the pattern. This is a typical situation where the transition occurs *via* a subcritical bifurcation. In this case, if one wants to predict the amplitude of the pattern, one needs to push the weakly nonlinear expansion at a higher order (for a general discussion on the relevance of the

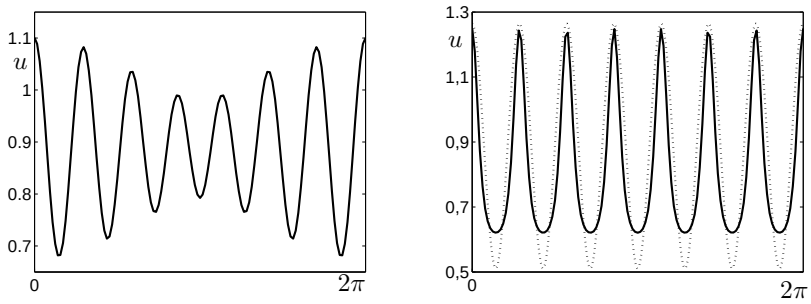

Fig. 3.6. *Left:* Initial condition $u = u_0 + \varepsilon(\bar{A}_1 \cos(k_1 x) + \bar{A}_2 \cos(k_2 x))$, where $\bar{A}_1 = 0.403, \bar{A}_2 = 0.405$ is in the basin of attraction of the equilibrium $(0, A_2)$. *Right:* The comparison between the expected solution $u = u_0 + \varepsilon A_2 \cos(k_2 x)$ (dotted line) and the numerical solution of the system (1.1) (solid line).

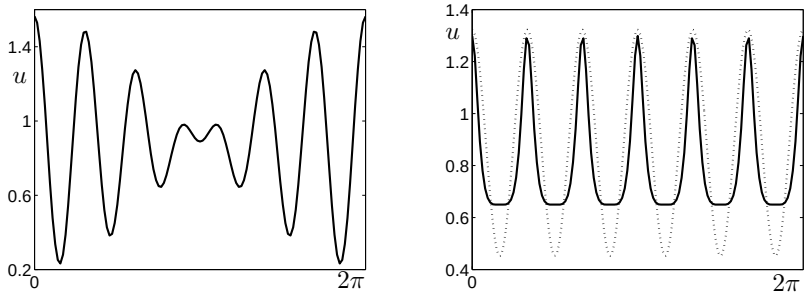

Fig. 3.7. *Left:* Initial condition $u = u_0 + \varepsilon(\bar{A}_1 \cos(k_1 x) + \bar{A}_2 \cos(k_2 x))$, where $\bar{A}_1 = 0.184, \bar{A}_2 = 0.071$ is in the basin of attraction of the equilibrium $(A_1, 0)$. *Right:* The comparison between the expected solution $u = u_0 + \varepsilon A_1 \cos(k_1 x)$ (dotted line) and the numerical solution of the system (1.1) (solid line).

higher order amplitude expansions in the study of subcritical bifurcations, see the recent [5] and references therein).

We introduce the multiple time scales T and T_1 as follows:

$$t = \frac{T}{\varepsilon^2} + \frac{T_1}{\varepsilon^4} + \cdots \tag{3.19}$$

and the following expansion of the bifurcation parameter:

$$b = b^c + \varepsilon^2 b^{(2)} + \varepsilon^4 b^{(4)} + O(\varepsilon^5)\,. \tag{3.20}$$

Performing the weakly nonlinear analysis up to $O(\varepsilon^5)$ one obtains the following quintic Stuart-Landau equation for the amplitude A:

$$\frac{dA}{dT} = \bar{\sigma} A - \bar{L} A^3 + \bar{Q} A^5\,. \tag{3.21}$$

The details of the analysis and the explicit expression of the coefficients appearing in (3.21) are given in Appendix C.

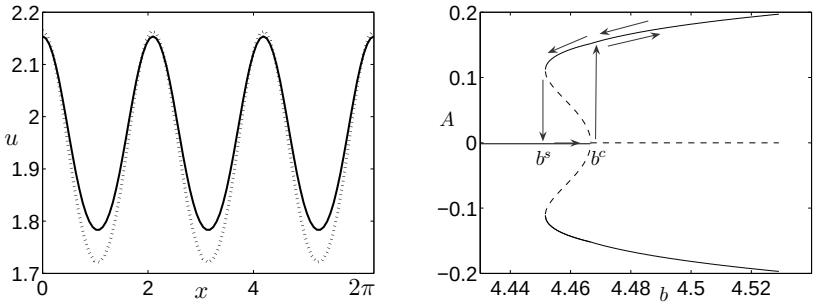

Fig. 3.8. The parameters are $\Gamma \approx 49.5$, $a_i = 0.1$, $c_i = 0.2$ $b_2 = 0.3$, $\mu_1 = 1.2$, $\mu_2 = 1$, $\gamma_{11} = 0.5$, $\gamma_{12} = 0.4$, $\gamma_{21} = 0.4$, $\gamma_{22} = 0.4$, $b^c \approx 4.4667$. *Left:* Comparison between the weakly nonlinear solution (solid line) and the numerical solution of (1.1) with $\epsilon \approx 0.1$ (dotted line). *Right:* The corresponding bifurcation diagram.

In the subcritical case, (i.e. when the growth rate coefficient $\bar{\sigma} > 0$ and the Landau coefficient $\bar{L} < 0$) and when $\bar{Q} < 0$, there exist two real stable equilibria representing the asymptotic values of the amplitude A. On the left of Fig. 3.8 we show a comparison between the numerical solution of the system (1.1) and the weakly nonlinear approximation.

On the right of Fig. 3.8 we show the bifurcation diagram for specific values of the parameters: the origin is locally stable for $b < b^c$ and, when $b = b^c$, two backward-bending branches of unstable fixed points bifurcate from the origin. These unstable branches turn around and become stable at some $b = b^s$ so that in the range $b^s < b < b^c$ two qualitatively different stable states coexist, namely the origin and the large amplitude branches. The existence of different stable states for one single value of the parameter allows for the possibility of hysteresis as b is varied. In Fig. 3.9 we show a hysteresis cycle corresponding to a periodic variation of the bifurcation parameter. Starting with a value of the parameter above b^c the solution jumps immediately to the stable branch corresponding to a pattern whose amplitude is relatively insensitive to the size of the bifurcation parameter. Decreasing b below the value b^c the solution persists on the upper branch and the pattern does not disappear. With a further decrease of b below b^s the solution jumps to the constant steady state. To have the pattern formation one has to increase the parameter b above b^c.

4 Traveling fronts

When the domain size is large a typical phenomenon one can observe is the propagation of the pattern through the physical domain in the form of a traveling wave: in this case the pattern is formed sequentially and the traveling wavefront is the precursor to patterning [38].

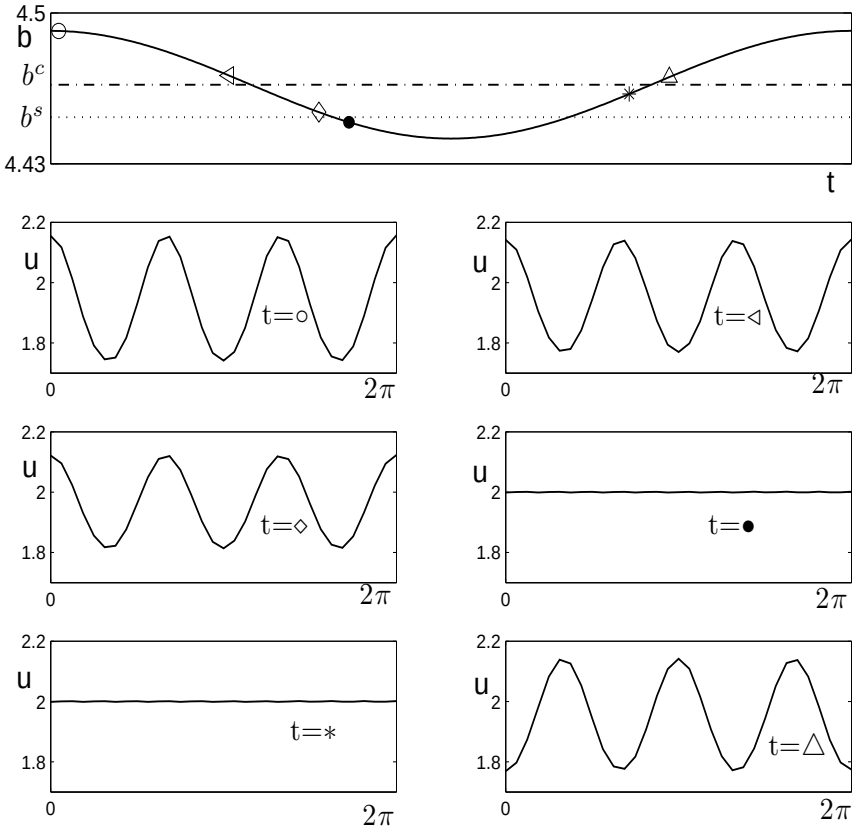

Fig. 3.9. A hysteresis cycle and the corresponding pattern evolution in the subcritical case. In the upper figure the variation in time of the bifurcation parameter $b = b^c + 0.025\cos(\omega t)$ with $\omega \approx 10^{-6}$. The values of the other parameters are the same as in Fig. 3.8.

To describe quantitatively this phenomenon one cannot ignore the (slow) modulation in space of the pattern amplitude, and one has to take into account the slow and the fast spatial dependence of the solution. One can easily see that, as typical for reaction diffusion systems [27], the characteristic length scale of spatial modulation (that we shall denote with X) is ε^{-1}.

The weakly nonlinear analysis of Section 3 must therefore be modified to keep into account the dependence of the amplitude A on X. Separating the fast x dependence and the slow X dependence, one can see that the spatial derivative decouples as $\partial_x \to \partial_x + \varepsilon\partial_X$ while the diffusion operator decouples as $\partial_{xx} \to \partial_{xx} + \varepsilon\partial_{xX} + \varepsilon^2\partial_{XX}$. At the lowest order ε we recover the linear problem $\mathcal{L}^{b^c}\mathbf{w}_1 = \mathbf{0}$ and the solution is:

$$\mathbf{w}_1 = A(X,T)\boldsymbol{\rho}\cos(k_c x)\ , \tag{4.1}$$

where $\boldsymbol{\rho}$ is given by (3.11). Pushing the asymptotic analysis (the details are not reproduced here) up to $O(\varepsilon^3)$ one finds the following equation for the amplitude A:

$$\frac{\partial A}{\partial T} = \nu \frac{\partial^2 A}{\partial X^2} + \sigma A - L A^3 \,, \tag{4.2}$$

where σ and L are given by (B.8) and (B.9). The diffusion coefficient ν is given by:

$$\nu = -\frac{< 2k_c D^{b^c} \mathbf{w}_{21} + D^{b^c} \boldsymbol{\rho}, \boldsymbol{\psi} >}{< \boldsymbol{\rho}, \boldsymbol{\psi} >} \,, \tag{4.3}$$

where $\boldsymbol{\psi}$ is given by (B.3).

The real Ginzburg-Landau (GL) equation (4.2) is able to capture the envelope evolution and the progressing of the pattern as a wave, as shown in Fig. 4.1. In the shown simulation, we have perturbed the equilibrium solution at the left end of the spatial interval. The parameters are the same as in Fig. 3.1 with $\varepsilon^2 = 0.1$, except $\Gamma = 2400$ which results in a $\bar{k}_c = 38$; we recall that to take Γ larger by a factor 30 is equivalent to have a spatial domain larger by a factor $\sqrt{30}$. After a transient, the solution of the system (1.1) assumes the form of a solution of the GL equation (modulated by $\cos(2\pi \bar{k}_c x)$), which is shown by the dashed line.

Notice also that the solution of the GL equation we show in the Figure (which is computed numerically imposing the Neumann boundary conditions), is very close to the following exact solution of the GL equation in $\mathbb{R}$:

$$A = \frac{1}{2}\sqrt{\frac{\sigma}{L}}\left(1 - \tanh\left(\sqrt{\frac{\sigma}{\nu}}\frac{z - z_0}{2\sqrt{2}}\right)\right), \quad \text{with } z = x - ct, \quad c = 3\sqrt{\frac{\sigma\nu}{2}} \,, \tag{4.4}$$

where the parameters σ, L and ν, are given by (B.8),(B.9) and (4.3).

5 Conclusions

In the present paper we have investigated the process of pattern formation induced by nonlinear cross-diffusion in a reaction-diffusion system with a simple kinetics of the competitive Lotka-Volterra type. We have determined the regions of the parameters space where the conditions for the diffusion driven instability are satisfied and the pattern emerges. Through a weakly nonlinear expansion, we have predicted the amplitude and the form of the pattern, deriving, both in the case of supercritical and subcritical bifurcation, the amplitude equations involving up to quintic order terms. In the parameters space we have also numerically identified the curves across which the bifurcation changes from supercritical to subcritical. Finally, we have considered the case

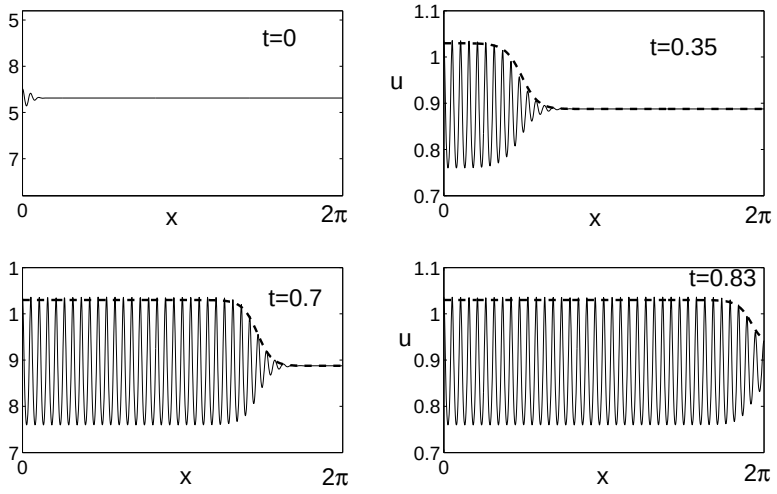

Fig. 4.1. When the perturbation of the equilibrium solution is localized, the pattern invades the whole domain in the form of a modulated progressing wave. The dashed line is a numerical solution of the GL equation (4.2), which is very close (when the front is distant from the boundaries) to the exact solution (4.4). The parameters are the same as in Fig. 3.1 (*Left*), except $\Gamma = 2400$.

of spatially modulated patterns, deriving the corresponding real Ginzburg-Landau amplitude equations. This has allowed us to describe the traveling front enveloping a pattern which invades a spatial domain.

All the predictions of the weakly nonlinear analysis are in good agreement with the numerical tests we have run, and both the cubic and the quintic amplitude equations give a correct bifurcation diagram close to criticality.

Several aspects of the problem remain to be examined. When the domain is two dimensional new phenomena occur. In fact, in this case degeneracy leads to more complex structures like rhombi, hexagons or mixed-modes patterns which may be predicted via the weakly nonlinear analysis [14], [23].

Moreover, experiments performed on real systems show deviations from the ideal patterns like boundary effects or the formation of localized structures (the so called defects). Far beyond the parameter regime where the amplitude equation is valid, defects play an important role on the pattern formation and the investigation of their dynamics is crucial to address the problem of pattern selection. In fact, while close to onset the defect dynamics can be addressed using competing amplitudes equation, far from threshold this approach fails: in this one dimensional case, where the defects are fronts, pulses, sources and sinks [48], the investigation of such topics would be of great interest.

Finally, non-stationary patterns should develop using a different form of the kinetic term (for example Lotka-Volterra predator-prey) coupled with attrac-

tive cross diffusion, of the type used e.g. in chemotaxis. This would cause the homogeneous state to lose its stability via a Hopf bifurcation and oscillating pattern would arise. These topics will be the subject of future work.

Acknowledgments

This work has been partially supported by INDAM and by the Department of Mathematics of the University of Palermo through the grant "Fondi di potenziamento della ricerca." We also thank the anonymous reviewers for several useful comments which helped significantly in improving the presentation of the paper.

A Pattern forming region in the parameter space

The goal of this Appendix is to give a geometric realization, in the parameter space, of the condition (2.8) which ensures the possibility of the pattern formation. First, to make the analysis simpler, and without loss of generality, we consider the following non dimensional form of the system (1.1):

$$\begin{aligned} \frac{\partial u}{\partial t} =& \Delta\left(u(c_1 + a_1 u + b v)\right) + \Gamma u\left(1 - u - \gamma_{12} v\right), \\ \frac{\partial v}{\partial t} =& \Delta\left(v(c_2 + a_2 v + b_2 u)\right) + \Gamma v\left(\mu_2 - \gamma_{21} u - v\right). \end{aligned} \tag{A.1}$$

Second we observe that the condition (2.8) involves the coefficients of the kinetics only. Therefore the parameter space to be considered is the three dimensional space $(\gamma_{12}, \gamma_{21}, \mu_2)$. In Fig. A.1 we show a two dimensional slice $\{\mu_2 = \text{const}\}$ of this space.

Third we observe that the conditions for the existence and the stability of the coexistence equilibrium point:

$$(u_0, v_0) \equiv \left(\frac{1 - \mu_2\gamma_{12}}{1 - \gamma_{12}\gamma_{21}}, \frac{\mu_2 - \gamma_{21}}{1 - \gamma_{12}\gamma_{21}}\right),$$

impose that

$$\gamma_{21} < \mu_2 \qquad \text{and} \quad \gamma_{12} < 1/\mu_2 \,. \tag{A.2}$$

The above condition, on the plane $\mu_2 = \text{const}$, corresponds to the region bounded by the rectangle shown in Fig. A.1. Notice also that the line $\gamma_{21} = \mu_2$ corresponds to $u_0 = 0$ while the line $\gamma_{12} = 1/\mu_2$ corresponds to $v_0 = 0$.

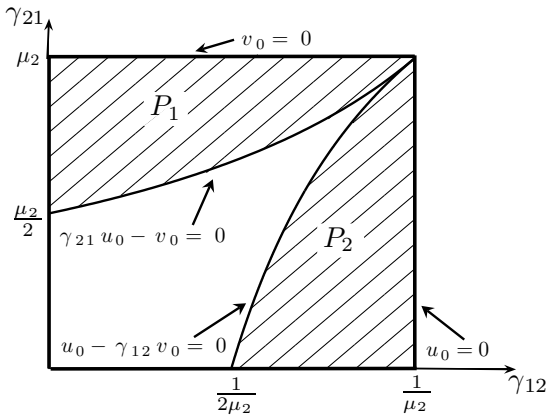

Fig. A.1. For fixed μ_2 the pattern forming regions in the plane $(\gamma_{12}, \gamma_{21})$ are the two hyperbolic sector P_1 and P_2.

We can finally impose the condition (2.8) which gives the two hyperbolic sectors, denoted by P_1 and P_2, in Fig. A.1.

B Derivation of the Stuart-Landau equation in 1D

Taking into account the solution at the lowest order given by (3.10), at $O(\varepsilon^2)$ we obtain the following equation:

$$\mathcal{L}^{b^c}\mathbf{w}_2 = \mathbf{F}\,, \tag{B.1}$$

with

$$\mathbf{F} = -\frac{1}{4}A^2 \sum_{i=0,2} \mathcal{M}_i(\boldsymbol{\rho},\boldsymbol{\rho})\cos(ik_c x), \tag{B.2}$$

where $\mathcal{M}_i = \mathcal{Q}_K - i^2 k_c^2 \mathcal{Q}_D^{b^c}$. By the Fredholm alternative, Eq.(B.1) admits a solution if and only if $< \mathbf{F}, \boldsymbol{\psi} >= 0$, where with $< \cdot, \cdot >$ we have denoted the scalar product in $L^2(0, 2\pi/k_c)$, and where $\boldsymbol{\psi} \in Ker\left\{\left(\Gamma K - k_c^2 D^{b^c}\right)^\dagger\right\}$. Since:

$$\boldsymbol{\psi} = \begin{pmatrix} 1 \\ M^* \end{pmatrix}\cos(k_c x), \qquad M^* = \frac{-D_{12}^{b^c}k_c^2 + \Gamma K_{12}}{D_{22}^{b^c}k_c^2 - \Gamma K_{22}}, \tag{B.3}$$

one immediately sees that the Fredholm alternative is automatically satisfied. The solution of the equation (B.1) is then explicitly computed in terms of the parameters of the full system:

$$\mathbf{w}_2 = A^2 \sum_{i=0,2} \mathbf{w}_{2i}\, \cos\left(ik_c x\right)), \tag{B.4}$$

where the vectors $\mathbf{w}_{2i}$ are the solutions of the following linear systems:

$$L_i \mathbf{w}_{2i} = -\frac{1}{4}\mathcal{M}_i(\boldsymbol{\rho}, \boldsymbol{\rho}), \qquad \text{for} \quad i = 0, 2 \tag{B.5}$$

with $L_i = \Gamma K - i^2 k_c^2 D^{b^c}$.

Equating the coefficients at $O(\varepsilon^3)$ gives the following equation:

$$\mathcal{L}^{b^c} \mathbf{w}_3 = \mathbf{G}, \tag{B.6a}$$

where

$$\mathbf{G} = \left(\frac{dA}{dT}\boldsymbol{\rho} + A\mathbf{G}_1^{(1)} + A^3\mathbf{G}_1^{(3)}\right)\cos(k_c x) + A^3\mathbf{G}_3\cos(3k_c x), \tag{B.6b}$$

and

$$\mathbf{G}_1^{(1)} = \begin{pmatrix} b^{(2)}k_c^2(Mu_0 + v_0) \\ 0 \end{pmatrix}, \tag{B.7a}$$

$$\mathbf{G}_1^{(3)} = -\mathcal{M}_1(\boldsymbol{\rho}, \mathbf{w}_{20}) - \frac{1}{2}\mathcal{M}_1(\boldsymbol{\rho}, \mathbf{w}_{22}), \tag{B.7b}$$

$$\mathbf{G}_3 = -\frac{1}{2}\mathcal{M}_3(\boldsymbol{\rho}, \mathbf{w}_{22}). \tag{B.7c}$$

The solvability condition $< \mathbf{G}, \boldsymbol{\psi} >= 0$ for the equation (B.6a) leads to (3.14), the Stuart-Landau equation for the amplitude $A(T)$, where the expressions of σ and L are given by:

$$\sigma = -\frac{< \mathbf{G}_1^{(1)}, \boldsymbol{\psi} >}{< \boldsymbol{\rho}, \boldsymbol{\psi} >}, \tag{B.8}$$

$$L = \frac{< \mathbf{G}_1^{(3)}, \boldsymbol{\psi} >}{< \boldsymbol{\rho}, \boldsymbol{\psi} >}. \tag{B.9}$$

In the pattern-forming region, shown in Fig. A.1, it is straightforward to prove that the coefficient σ is always positive. On the other hand, within the region labeled P_1, L can be positive or negative depending on the values of the system parameters. We recall that if L is positive (negative) on has a supercritical (subcritical) bifurcation.

The expression for L as a function of all the parameters is quite involved. It is therefore hard to perform a general analytical study of the sign of the Landau constant.

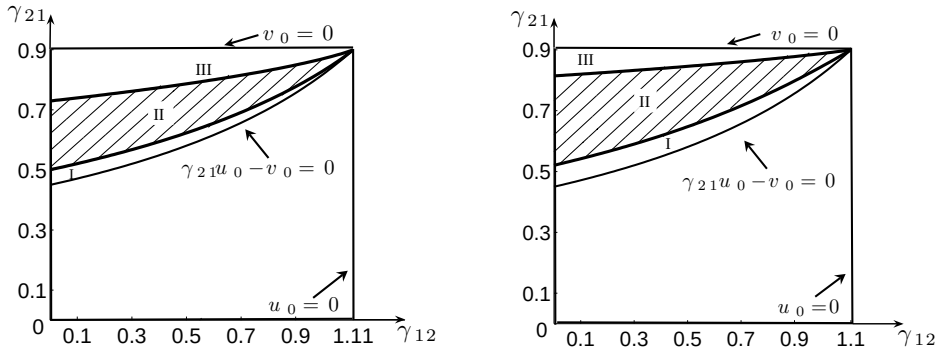

Fig. B.1. Within the pattern forming region, the zones of subcritical (I and III) and supercritical (II, dashed) bifurcation are drawn. The parameters are $\Gamma = 50$, $\mu_2 = 0.9$, $a_2 = 0.01$, $b_2 = 0.3$, $c_i = 0.1$. *Left:* $a_1 = 0.02$. *Right:* $a_1 = 5$.

Here we present a couple of examples where (keeping fixed all the other parameters, and using the non dimensional form of the system (A.1)) we draw, in the space $(\gamma_{12}, \gamma_{21})$, the curves across which L changes its sign (see Fig. B.1). These curves have been determined numerically. On the left of Fig. B.1 one can see that in the pattern forming region P_1 there are two curves across which L changes sign. If $(\gamma_{12}, \gamma_{21})$ are chosen in region II (dashed) one has the supercritical bifurcation, while regions I and III correspond to the subcritical case.

The effect of changing the values of the diffusion parameters is to shift upwards the boundaries between the regions. In particular, on the right of Fig. B.1 we show the effect of increasing the value of the parameter a_1. A qualitatively analogous phenomenon occurs when one increases the values of c_i and a_2.

In all cases we have considered we have always seen the same qualitative picture: two subcritical bifurcation regions close to the boundary of the pattern forming region, and one supercritical bifurcation region in between.

C The quintic Stuart–Landau equation

In this Appendix we give the details of the derivation of the quintic Stuart-Landau equation (3.21).

Substituting the expansions (3.19), (3.20) and (3.6) into (3.1), the resulting equations, up to $O(\varepsilon^3)$, are the same we have presented in Section 3.

Taking into account that (3.14) still holds for the amplitude $A(T, T_1)$ (although now the derivative with respect to T is a partial derivative), the solvability

condition $< \mathbf{G}, \psi >= 0$ for (3.13) is satisfied and the solution is:

$$\mathbf{w}_3 = \left(A\mathbf{w}_{31} + A^3\mathbf{w}_{32}\right)\cos\left(k_c x\right) + A^3\mathbf{w}_{33}\cos\left(3k_c x\right), \tag{C.1}$$

where the expression for the vectors $\mathbf{w}_{3i}, i = 1, 2, 3$ can be computed solving the following linear systems:

$$\begin{aligned}
L_1\mathbf{w}_{31} &= \sigma\boldsymbol{\rho} + \mathbf{G}_1^{(1)} \\
L_2\mathbf{w}_{32} &= -L\boldsymbol{\rho} + \mathbf{G}_1^{(3)} \\
L_3\mathbf{w}_{33} &= \mathbf{G}_3
\end{aligned}$$

where we have defined $L_i = \Gamma K - i^2 k_c^2 D^{b^c}$ and $\mathbf{G}_1^{(1)}, \mathbf{G}_1^{(3)}, \mathbf{G}_3$ are given in formula (B.7).

At $O(\varepsilon^4)$ the resulting equation is:

$$\mathcal{L}^{b^c}\mathbf{w}_4 = \mathbf{H}, \tag{C.2}$$

where:

$$\begin{aligned}
\mathbf{H} = {} & 2A\frac{\partial A}{\partial T}\mathbf{w}_{20} + A^2\mathbf{H}_0^{(2)} + A^4\mathbf{H}_0^{(4)} + \\
& \left(2A\frac{\partial A}{\partial T}\mathbf{w}_{22} + A^2\mathbf{H}_2^{(2)} + A^4\mathbf{H}_2^{(4)}\right)\cos(2k_c x) + A^4\mathbf{H}_4\cos(4k_c x),
\end{aligned} \tag{C.3}$$

and

$$\begin{aligned}
\mathbf{H}_0^{(2)} &= -\frac{1}{2}\,\mathcal{Q}_K(\boldsymbol{\rho}, \mathbf{w}_{31}), \\
\mathbf{H}_0^{(4)} &= -\mathcal{Q}_K(\mathbf{w}_{20}, \mathbf{w}_{20}) - \frac{1}{4}\mathcal{Q}_K(\mathbf{w}_{22}, \mathbf{w}_{22}) - \frac{1}{2}\mathcal{Q}_K(\boldsymbol{\rho}, \mathbf{w}_{22}), \\
\mathbf{H}_2^{(2)} &= -\frac{1}{2}\mathcal{M}_2(\boldsymbol{\rho}, \mathbf{w}_{31}) + \begin{pmatrix} 4b^{(2)}k_c^2\left(u_0 w_{22}^v + v_0 w_{22}^u + M/2\right) \\ 0 \end{pmatrix}, \\
\mathbf{H}_2^{(4)} &= -\frac{1}{2}\mathcal{M}_2(\boldsymbol{\rho}, \mathbf{w}_{32}) - \frac{1}{2}\mathcal{M}_2(\boldsymbol{\rho}, \mathbf{w}_{33}) - \mathcal{M}_2(\mathbf{w}_{20}, \mathbf{w}_{20}), \\
\mathbf{H}_4 &= -\frac{1}{2}\mathcal{M}_4(\boldsymbol{\rho}, \mathbf{w}_{33}) - \frac{1}{4}\mathcal{M}_4(\mathbf{w}_{22}, \mathbf{w}_{22}).
\end{aligned}$$

The solvability condition for (C.2) is automatically satisfied and the solution is:

$$\mathbf{w}_4 = A^2\mathbf{w}_{40} + A^4\mathbf{w}_{41} + \left(A^2\mathbf{w}_{42} + A^4\mathbf{w}_{43}\right)\cos(2k_c x) + A^4\mathbf{w}_{44}\cos(4k_c x), \tag{C.4}$$

where the vector $\mathbf{w}_{4i}$, $i = 1, \ldots, 4$, are the solutions of the following linear systems:

$$
\begin{aligned}
\Gamma K \mathbf{w}_{40} &= 2\sigma \mathbf{w}_{20} + \mathbf{H}_0^{(2)} \\
\Gamma K \mathbf{w}_{41} &= -2L \mathbf{w}_{20} + \mathbf{H}_0^{(4)} \\
L_2 \mathbf{w}_{42} &= 2\sigma \mathbf{w}_{22} + \mathbf{H}_2^{(2)} \\
L_3 \mathbf{w}_{43} &= -2L \mathbf{w}_{22} + \mathbf{H}_2^{(4)} \\
L_4 \mathbf{w}_{44} &= \mathbf{H}_4
\end{aligned}
$$

At $O(\varepsilon^5)$ the resulting equation is:

$$
\mathcal{L}^{b^c} \mathbf{w}_5 = \mathbf{P}\,, \tag{C.5}
$$

where:

$$
\begin{aligned}
\mathbf{P} = &\left(\frac{\partial A}{\partial T_1} \boldsymbol{\rho} + \frac{\partial A}{\partial T} \mathbf{w}_{31} + 3A^2 \frac{\partial A}{\partial T} \mathbf{w}_{32} + A \mathbf{P}_1^{(1)} + A^3 \mathbf{P}_1^{(3)} + A^5 \mathbf{P}_1^{(5)} \right) \cos(k_c x) \\
&+ \left(3A^2 \frac{\partial A}{\partial T} \mathbf{w}_{33} + A^3 \mathbf{P}_3^{(3)} + A^3 \mathbf{P}_3^{(5)} \right) \cos(3k_c x) + A^5 \mathbf{P}_5 \cos(5k_c x)
\end{aligned} \tag{C.6}
$$

and

$$
\begin{aligned}
\mathbf{P}_1^{(1)} =& \begin{pmatrix} b^{(2)}k_c^2\left(u_0 w_{31}^v + v_0 w_{31}^u\right) + b^{(4)}k_c^2\left(u_0 M + v_0\right) \\ 0 \end{pmatrix}, \\
\mathbf{P}_1^{(3)} =& -\mathcal{M}_1(\boldsymbol{\rho}, \mathbf{w}_{40}) - \frac{1}{2}\mathcal{M}_1(\boldsymbol{\rho}, \mathbf{w}_{42}) - \mathcal{M}_1(\mathbf{w}_{20}, \mathbf{w}_{31}) - \frac{1}{2}\mathcal{M}_1(\mathbf{w}_{22}, \mathbf{w}_{31}) \\
&+ \begin{pmatrix} b^{(2)}k_c^2\left(u_0 w_{32}^v + v_0 w_{32}^u + w_{20}^v + \frac{w_{22}^v}{2} + M(w_{20}^u + \frac{w_{22}^u}{2})\right) \\ 0 \end{pmatrix}, \\
\mathbf{P}_1^{(5)} =& -\mathcal{M}_1(\boldsymbol{\rho}, \mathbf{w}_{41}) - \frac{1}{2}\mathcal{M}_1(\boldsymbol{\rho}, \mathbf{w}_{431}) - \mathcal{M}_1(\mathbf{w}_{20}, \mathbf{w}_{32}) \\
&-\frac{1}{2}\mathcal{M}_1(\mathbf{w}_{22}, \mathbf{w}_{32}) - \frac{1}{2}\mathcal{M}_1(\mathbf{w}_{22}, \mathbf{w}_{33}), \\
\mathbf{P}_3^{(3)} =& -\frac{1}{2}\mathcal{M}_3(\boldsymbol{\rho}, \mathbf{w}_{42}) - \frac{1}{2}\mathcal{M}_3(\mathbf{w}_{22}, \mathbf{w}_{31}) \\
&+ \begin{pmatrix} 9b^{(2)}k_c^2\left(u_0 w_{33}^v + v_0 w_{33}^u + \frac{1}{2}w_{22}^v + \frac{1}{2}M w_{22}^u\right) \\ 0 \end{pmatrix}, \\
\mathbf{P}_3^{(5)} =& -\frac{1}{2}\mathcal{M}_3(\boldsymbol{\rho}, \mathbf{w}_{44}) - \frac{1}{2}\mathcal{M}_3(\boldsymbol{\rho}, \mathbf{w}_{43}) - \frac{1}{2}\mathcal{M}_3(\mathbf{w}_{22}, \mathbf{w}_{32}), \\
\mathbf{P}_5 =& -\frac{1}{2}\mathcal{M}_5(\boldsymbol{\rho}, \mathbf{w}_{44}) - \frac{1}{2}\mathcal{M}_5(\mathbf{w}_{22}, \mathbf{w}_{33}).
\end{aligned}
$$

The solvability condition for (C.5) is

$$
\frac{\partial A}{\partial T_1} = \tilde{\sigma} A - \tilde{L} A^3 + \tilde{Q} A^5, \tag{C.7}
$$

where the coefficients are given by:

$$
\begin{aligned}
\tilde{\sigma} =& -\frac{< \sigma \mathbf{w}_{31} + \mathbf{P}_1^{(1)}, \boldsymbol{\psi} >}{< \boldsymbol{\rho}, \boldsymbol{\psi} >}, \\
\tilde{L} =& \frac{< 3\sigma \mathbf{w}_{32} - L\mathbf{w}_{31} + \mathbf{P}_1^{(3)}, \boldsymbol{\psi} >}{< \boldsymbol{\rho}, \boldsymbol{\psi} >}, \\
\tilde{Q} =& \frac{< 3L\mathbf{w}_{32} - \mathbf{P}_1^{(5)}, \boldsymbol{\psi} >}{< \boldsymbol{\rho}, \boldsymbol{\psi} >}.
\end{aligned} \tag{C.8}
$$

Adding up (C.7) to (3.14) one gets the quintic Stuart-Landau equation (3.21) with:

$$
\bar{\sigma} = \sigma + \varepsilon^2 \tilde{\sigma}, \qquad \bar{L} = L + \varepsilon^2 \tilde{L}, \qquad \bar{Q} = \tilde{Q}\varepsilon^2. \tag{C.9}
$$

D Nonlinear behavior of two competing modes

Let us assume that both the modes k_1 and k_2 become unstable. Performing the weakly nonlinear analysis, one can write the solution of the linear problem at $O(\varepsilon)$ in (3.10) as:

$$\mathbf{w}_1 = \sum_{l=1}^{2} A_l \boldsymbol{\rho}_l \cos(k_l x), \quad \text{where } \boldsymbol{\rho}_l = \begin{pmatrix} 1 \\ M_l \end{pmatrix}, \; M_l = \frac{-D_{21}^{b^c} k_l^2 + \Gamma K_{21}}{D_{22}^{b^c} k_l^2 - \Gamma K_{21}}.$$

Upon the substitution of the above expression into (3.12), the vector $\mathbf{F}$ reads:

$$\begin{aligned} \mathbf{F} = &-\frac{1}{4} \sum_{l=1}^{2} A_l^2 \sum_{\substack{i=0 \\ i \neq 1}}^{2} \mathcal{M}_i^l(\boldsymbol{\rho}_l, \boldsymbol{\rho}_l) \cos(i k_l x) \\ &-\frac{1}{2} A_1 A_2 \left(\mathcal{M}_p(\boldsymbol{\rho}_1, \boldsymbol{\rho}_2) \cos((k_1 + k_2)x) + \mathcal{M}_m(\boldsymbol{\rho}_1, \boldsymbol{\rho}_2) \cos((k_1 - k_2)x) \right), \end{aligned} \tag{D.1}$$

where $\mathcal{M}_i^l = \mathcal{Q}_K - i^2 k_l^2 \mathcal{Q}_D^{b^c}$, $\mathcal{M}_p = \mathcal{Q}_K - (k_1 + k_2)^2 \mathcal{Q}_D^{b^c}$ and $\mathcal{M}_m = \mathcal{Q}_K - (k_1 - k_2)^2 \mathcal{Q}_D^{b^c}$.

The terms in (D.1) identically satisfy the compatibility conditions and the solution of (3.13) is then calculated:

$$\mathbf{w}_2 = \sum_{l=1}^{2} A_l^2 \sum_{\substack{i=0 \\ i \neq 1}}^{2} \mathbf{w}_{2i}^l \cos(i k_l x) + A_1 A_2 (\mathbf{w}_{2p} \cos((k_1 + k_2)x) + \mathbf{w}_{2m} \cos((k_1 - k_2)x)). \tag{D.2}$$

where the vectors $\mathbf{w}_{2i}^l, \mathbf{w}_p$ and $\mathbf{w}_m$ are the solutions to the following linear systems:

$$\begin{aligned} L_i^l \mathbf{w}_{2i}^l &= -\frac{1}{4} \mathcal{M}_i^l(\boldsymbol{\rho}_l, \boldsymbol{\rho}_l), \\ L_p \mathbf{w}_{2p} &= -\frac{1}{2} \mathcal{M}_p(\boldsymbol{\rho}_1, \boldsymbol{\rho}_2), \\ L_m \mathbf{w}_{2m} &= -\frac{1}{2} \mathcal{M}_m(\boldsymbol{\rho}_1, \boldsymbol{\rho}_2), \end{aligned}$$

and the operators L_i^l, L_p and L_m are defined as follows:

$$\begin{aligned} L_i^l &= \Gamma K - i^2 k_l^2 D^{b^c}, \\ L_p &= \Gamma K - (k_1 + k_2)^2 D^{b^c}, \\ L_m &= \Gamma K - (k_1 - k_2)^2 D^{b^c}. \end{aligned}$$

At order ε^3 the expression of the vector $\mathbf{G}$, which appears in the formula (3.13) reads:

$$\mathbf{G} = \sum_{l=1}^{2} \left(\frac{dA_l}{dT_2} \boldsymbol{\rho}_l + A_l \mathbf{G}_1^{(1)l} + A_l^3 \mathbf{G}_1^{(3)l} + \frac{A_1^2 A_2^2}{A_l} \mathbf{G}_1^l \right) \cos(k_l x) + \mathbf{G}^* \,, \qquad \text{(D.3)}$$

where:

$$\begin{aligned} \mathbf{G}_1^{(1)l} &= b^{(2)} k_l^2 \begin{pmatrix} u_0 M_l + v_0 \\ 0 \end{pmatrix}, \\ \mathbf{G}_1^{(3)l} &= -\left(\mathcal{M}_1^l(\boldsymbol{\rho}_l, \mathbf{w}_{20}^l) + \frac{1}{2} \mathcal{M}_1^l(\boldsymbol{\rho}_l, \mathbf{w}_{22}^l) \right), \\ \mathbf{G}_1^l &= -\left(\mathcal{M}_1^l(\boldsymbol{\rho}_l, \mathbf{w}_{20}^{2/l} + \frac{1}{2} \mathcal{M}_1^l(\boldsymbol{\rho}_l, \mathbf{w}_{2p}) + \frac{1}{2} \mathcal{M}_1^l(\boldsymbol{\rho}_l, \mathbf{w}_{2m}) \right). \end{aligned}$$

and the expression of $\mathbf{G}^*$ involves only terms orthogonal to $\boldsymbol{\psi}$ so we shall not report it here.

By imposing the solvability condition to the equation (3.13), we obtain the Landau equations (3.18a)-(3.18b) for the amplitudes $A_1(T_2)$ and $A_2(T_2)$. The expressions for the coefficients appearing in these equations are given below:

$$\sigma_l = -\frac{< \mathbf{G}_1^{(1)l}, \boldsymbol{\psi}_l >}{< \boldsymbol{\rho}_l, \boldsymbol{\psi}_l >}, \qquad \text{(D.4)}$$

$$L_l = \frac{< \mathbf{G}_1^{(3)l}, \boldsymbol{\psi}_l >}{< \boldsymbol{\rho}_l, \boldsymbol{\psi}_l >}, \qquad \text{(D.5)}$$

$$\Omega_l = -\frac{< \mathbf{G}_1^{l}, \boldsymbol{\psi}_l >}{< \boldsymbol{\rho}_l, \boldsymbol{\psi}_l >}. \qquad \text{(D.6)}$$

References

[1] Y. Almirantis, S. Papageorgiou, Cross-diffusion effects on chemical and biological pattern formation, J. Theor. Biol. 151 (1991) 289–311.

[2] M. Andreianov, B. Bendahmane, R. Ruiz-Baier, Analysis of a finite volume method for a cross-diffusion model in population dynamics, Math. Mod. Meth. Appl. Sci. 21 (2) (2011) 307–344.

[3] I. S. Aranson, L. S. Tsimring, Continuum theory of partially fluidized granular flows, Phys. Rev. E (3) 65 (6) (2002) 061303, 20.

[4] J. W. Barrett, J. F. Blowey, Finite element approximation of a nonlinear cross-diffusion population model, Numer. Math. 98 (2) (2004) 195–221.

[5] P. Becherer, A. N. Morozov, W. van Saarloos, Probing a subcritical instability with an amplitude expansion: An exploration of how far one can get, Physica D 238 (18) (2009) 1827–1840.

[6] N. Ben Abdallah, P. Degond, S. Genieys, An energy-transport model for semiconductors derived from the Boltzmann equation, J. Statist. Phys. 84 (1-2) (1996) 205–231.

[7] S. Berres, R. Ruiz-Baier, A fully adaptive numerical approximation for a two-dimensional epidemic model with nonlinear cross-diffusion, Nonlinear Analysis: Real World Applications 12 (5) (2011) 2888–2903.

[8] L. Chen, A. Jüngel, Analysis of a multidimensional parabolic population model with strong cross-diffusion, SIAM J. Math. Anal. 36 (1) (2004) 301–322.

[9] L. Chen, A. Jüngel, Analysis of a parabolic cross–diffusion population model without self–diffusion, J. Differential Equations 224 (1) (2006) 39–59.

[10] L. Chen, A. Jüngel, Analysis of a parabolic cross-diffusion semiconductor model with electron-hole scattering, Comm. Partial Differential Equations 32 (1-3) (2007) 127–148.

[11] F. Conforto, L. Desvillettes, Rigorous passage to the limit in a system of reaction-diffusion equations towards a system including cross diffusions, preprint (2009).

[12] P. H. Coullet, E. A. Spiegel, Amplitude equations for systems with competing instabilities, SIAM J. Appl. Math. 43 (4) (1983) 776–821.

[13] M. Cross, H. Greenside, Pattern Formation and Dynamics in Nonequilibrium Systems, Cambridge University Press, Cambridge, 2009.

[14] G. C. Cruywagen, P. K. Maini, J. D. Murray, Biological pattern formation on two-dimensional spatial domains: a nonlinear bifurcation analysis, SIAM J. Appl. Math. 57 (6) (1997) 1485–1509.

[15] P. Degond, S. Génieys, A. Jüngel, A system of parabolic equations in nonequilibrium thermodynamics including thermal and electrical effects, J. Math. Pures Appl. (9) 76 (10) (1997) 991–1015.

[16] D. del Castillo-Negrete, B. A. Carreras, Front propagation and segregation in a reaction-diffusion model with cross-diffusion, Phys. Plasmas 9 (2002) 118–127.

[17] D. del Castillo-Negrete, B. A. Carreras, V. Lynch, Front propagation and segregation in a reaction-diffusion model with cross-diffusion, Phys. D 168/169 (2002) 45–60.

[18] J. M. Epstein, Nonlinear Dynamics, Mathematical Biology and Social Science, Addison-Wesley, Reading, MA, 1997.

[19] G. Galiano, Modeling spatial adaptation of populations by a time non-local convection cross-diffusion evolution problem, Applied Mathematics and Computation 218 (8) (2011) 4587 – 4594.

[20] G. Galiano, M. L. Garzón, A. Jüngel, Semi-discretization in time and numerical convergence of solutions of a nonlinear cross-diffusion population model, Numer. Math. 93 (4) (2003) 655–673.

[21] G. Galiano, A. Jüngel, J. Velasco, A parabolic cross-diffusion system for granular materials, SIAM J. Math. Anal. 35 (3) (2003) 561–578 (electronic).

[22] G. Galiano, J. Velasco, Competing through altering the environment: a cross–diffusion population model coupled to transport–Darcy flow equations, Nonlinear Analysis: Real World Applications 12 (2011) 2826–2838.

[23] G. Gambino, M. C. Lombardo, M. Sammartino, Pattern formation driven by cross–diffusion in a 2D domain, *in preparation*.

[24] G. Gambino, M. C. Lombardo, M. Sammartino, Cross-diffusion driven instability for a Lotka-Volterra competitive reaction-diffusion system, in: "WASCOM 2007"—14th Conference on Waves and Stability in Continuous Media, World Sci. Publ., Hackensack, NJ, 2008, pp. 297–302.

[25] G. Gambino, M. C. Lombardo, M. Sammartino, A velocity-diffusion method for a Lotka-Volterra system with nonlinear cross and self-diffusion, Appl. Numer. Math. 59 (5) (2009) 1059–1074.

[26] E. Gilad, J. von Hardenberg, A. Provenzale, M. Shachak, E. Meron, A mathematical model of plants as ecosystem engineers, J. Theoret. Biol. 244 (4) (2007) 680–691.

[27] M. van Hecke, P. Hohenberg, W. van Saarloos, Amplitude equations for pattern forming systems, in: H. van Beijeren, M. Ernst (eds.), Fundamental Problems in Statistical Mechanics VIII, North-Holland, Amsterdam, 1994, pp. 245–278.

[28] B. I. Henry, S. L. Wearne, Existence of Turing instabilities in a two-species reaction-diffusion system, SIAM J. Appl. Math. 62 (3) (2002) 870–887.

[29] R. Hoyle, Pattern Formation. An Introduction to Methods, Cambridge University Press, Cambridge, 2006.

[30] M. Iida, M. Mimura, H. Ninomiya, Diffusion, cross-diffusion and competitive interaction, J. Math. Biol. 53 (4) (2006) 617–641.

[31] K. Kishimoto, H. F. Weinberger, The spatial homogeneity of stable equilibria of some reaction-diffusion systems on convex domains, J. Differential Equations 58 (1) (1985) 15–21.

[32] R. Kohn, Energy-driven pattern formation, in: Proceedings of the International Congress of Mathematicians, European Mathematical Society, Madrid, 2006, pp. 1–25.

[33] L. Landau, On the problem of turbulence, Dokl. Akad. Nauk SSSR 44 (1944) 311–314.

[34] D. Lauffenburger, R. Aris, K. Keller, Effects of cell motility and chemotaxis on microbial population growth, Biophys. J. 40 (1982) 209–219.

[35] Y. Lou, W. M. Ni, Diffusion, self-diffusion and cross-diffusion, J. Differential Equations 131 (1) (1996) 79–131.

[36] Y. Lou, W. M. Ni, S. Yotsutani, On a limiting system in the Lotka-Volterra competition with cross-diffusion. Partial differential equations and applications, Discrete Contin. Dyn. Syst. 10 (1-2) (2004) 435–458.

[37] M. Mimura, K. Kawasaki, Spatial segregation in competitive interaction-diffusion equations, J. Math. Biol. 9 (1) (1980) 49–64.

[38] J. D. Murray, Mathematical Biology, vol. I & II, 3rd ed., Springer, New York, 2007.

[39] R. A. Satnoianu, M. Menzinger, P. K. Maini, Turing instability in general systems, J. Math. Biol. 41 (6) (2000) 493–512.

[40] L. Segel, Modeling dynamic phenomena in molecular and cellular biology, 2nd ed., Cambridge University Press, New York, 1987.

[41] L. A. Segel, The non-linear interaction of two disturbances in the thermal convection problem, J. Fluid Mech. 14 (1962) 97–114.

[42] L. A. Segel, The non-linear interaction of a finite number of disturbances to a layer of fluid heated from below, J. Fluid Mech. 21 (1965) 359–384.

[43] J. A. Sherratt, Wavefront propagation in a competition equation with a new motility term modelling contact inhibition between cell populations, R. Soc. Lond. Proc. Ser. A Math. Phys. Eng. Sci. 456 (2002) (2000) 2365–2386.

[44] N. Shigesada, K. Kawasaki, E. Teramoto, Spatial segregation of interacting species, J. Theo. Biology 79 (1979) 83–99.

[45] C. Tian, Turing patterns created by cross-diffusion for a Holling II and Leslie-Gower type three species food chain model, Journal of Mathematical Chemistry 49 (2011) 1128–1150.

[46] C. Tian, Z. Lin, M. Pedersen, Instability induced by cross-diffusion in reaction-diffusion systems, Nonlinear Analysis: Real World Applications 11 (2010) 1036–1045.

[47] A. M. Turing, The chemical basis of morphogenesis, Phil. Trans. Roy. Soc. London, B 237 (1952) 37–72.

[48] W. van Saarloos, P. Hohenberg, Fronts, pulses, sources and sinks in generalized complex Ginzburg-Landau equations, Physica D 56 (1992) 303–367.

[49] V. K. Vanag, I. R. Epstein, Cross-diffusion and pattern formation in reaction-diffusion systems, Phys. Chem. Chem. Phys. 11 (2009) 897–912.

[50] D. J. Wollkind, V. S. Manoranjan, L. Zhang, Weakly nonlinear stability analyses of prototype reaction-diffusion model equations, SIAM Rev. 36 (2) (1994) 176–214.

[51] H. Yizhaq, B. Portnov, E. Meron, A mathematical model of segregation patterns in residential neighbourhoods, Environment and Planning A 36 (2004) 149 – 172.

[52] J. Zhang, W. Li, Y. Wang, Turing patterns of a strongly coupled predator-prey system with diffusion effects, Nonlinear Analysis 74 (2011) 847 – 858.